Charge Transport Layers Limiting the Efficiency of Perovskite Solar Cells: How To Optimize Conductivity, Doping, and Thickness

Vincent M. Le Corre,[*,†] Martin Stolterfoht,[‡] Lorena Perdigón Toro,[‡] Markus Feuerstein,[‡] Christian Wolff,[‡] Lidón Gil-Escrig,[§,∥] Henk J. Bolink,[§] Dieter Neher,[‡] and L. Jan Anton Koster[*,†]

†Zernike Institute for Advanced Materials, University of Groningen, Nijenborgh 4, 9747 AG Groningen, The Netherlands
‡Institute of Physics and Astronomy, University of Potsdam, 14476 Potsdam, Germany
§Instituto de Ciencia Molecular, Universidad de Valencia, C/J. Beltrán 2, 46980 Paterna, Spain

Ⓢ Supporting Information

ABSTRACT: Perovskite solar cells (PSCs) are one of the main research topics of the photovoltaic community; with efficiencies now reaching up to 24%, PSCs are on the way to catching up with classical inorganic solar cells. However, PSCs have not yet reached their full potential. In fact, their efficiency is still limited by nonradiative recombination, mainly via trap-states and by losses due to the poor transport properties of the commonly used transport layers (TLs). Indeed, state-of-the-art TLs (especially if organic) suffer from rather low mobilities, typically within 10^{-5} and 10^{-2} cm^2 V^{-1} s^{-1}, when compared to the high mobilities, $1-10$ cm^2 V^{-1} s^{-1}, measured for perovskites. This work presents a comprehensive analysis of the effect of the mobility, thickness, and doping density of the transport layers based on combined experimental and modeling results of two sets of devices made of a solution-processed high-performing triple-cation (PCE ≈ 20%). The results are also cross-checked on vacuum-processed MAPbI$_3$ devices. From this analysis, general guidelines on how to optimize a TL are introduced and especially a new and simple formula to easily calculate the amount of doping necessary to counterbalance the low mobility of the TLs.

KEYWORDS: perovskite solar cells, transport layers, conductivity, doping, charge transport
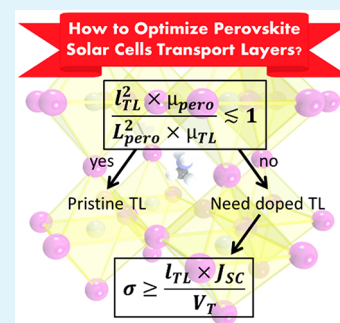
Perovskite solar cells (PSCs) have attracted more and more attention in the photovoltaic research community. The number of published articles on PSCs keeps increasing whereas the yearly number of publications even tripled between 2015 and 2017. Following the trend of the number of published papers, the efficiency of perovskite solar cells also skyrocketed within less than 10 years from 3.8%[1] to 24%.[2] The first jump in efficiency was linked to the establishment of solid-state perovskite solar cells,[3,4] as opposed to the dye-sensitized structure previously used.[1] From this point, the incredibly fast development of PSCs is due to optimization efforts on several levels: (1) The deposition techniques highly improved leading to better film quality, i.e., less rough and more compact with bigger grains.[5−7] (2) The chemical engineering of the perovskite by using mixed-compound (cations, metal and/or halide) allowed band gap tunability and improvement of the stability.[8−11] (3) The solar cell stack was optimized by choosing more suitable charge-selective transport layers (TLs).[10,12−23]

As the perovskite layer quality improved, the focus shifted to the optimization of the TLs. Classical PSCs consist of a simple $n-i-p$ or $p-i-n$ structure, where the perovskite layer is stacked between two TLs and electrodes. In principle, an efficient TL must fulfill several aspects which include (a) a favorable energy level alignment, for a good transfer of one type of charge carrier while effectively blocking the other;[24−26]

(b) good chemical and physical properties, to avoid detrimental reactions with the surrounding layers and the environment, and also suitable surface properties[27] as these two points could otherwise result in a significant amount of traps at the interface and/or a poor perovskite layer quality (rough or too many grain boundaries) when grown on top of the TL; (c) high transparency of the TLs to maximize the absorption in the perovskite layer;[28] and finally (d) good transport properties to ensure a fast transport of the charge carriers toward the extracting electrode.[28,29]

This study will focus on the last point (d) as most of the state-of-the-art TLs suffer from a rather low mobility compared to the perovskite. Theoretical calculations on the perovskite structure give mobility values ranging from several hundred to thousands of cm^2 V^{-1} s^{-1}.[30] However, the usual electrical techniques, such as field-effect transistor measurement or space-charge-limited-current, report mobilities which are orders of magnitude lower on the range of 1 to several tens of cm^2 V^{-1} s^{-1}.[15,17,30,31] In any case the perovskite mobility is higher than that of most TLs and can therefore limit the efficiency.
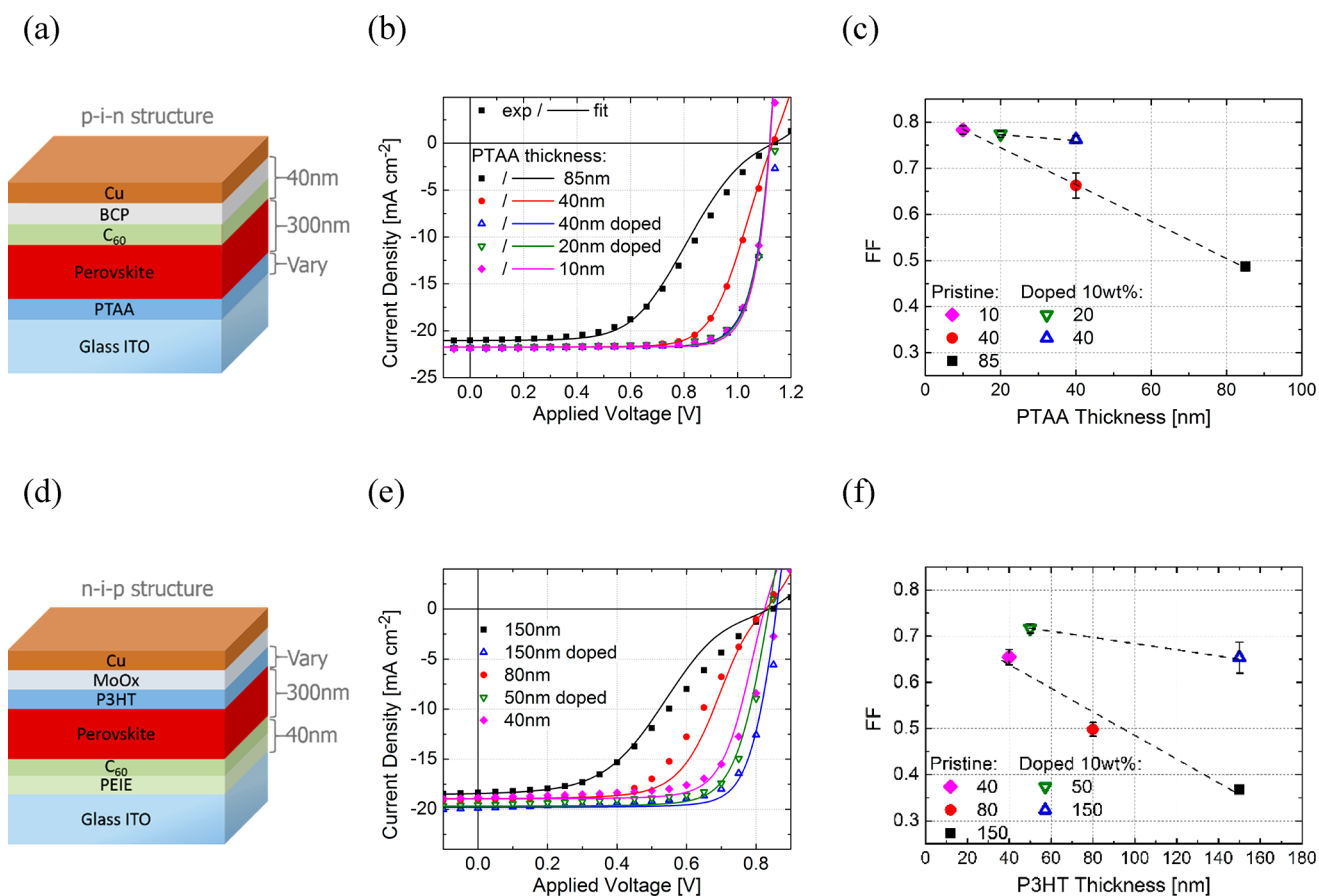
Figure 1. (a, d) Schematic of the device structures investigated. (b, e) Current density versus voltage characteristics of the solar cells for different HTL thicknesses and doping; the dots correspond to the experiment, and the line corresponds to the numerical fit. The fitting parameters can be found in the SI. (c, f) The FF of the two devices linearly depends on the HTL thickness but is also strongly enhanced by doping; filled dots correspond to the pristine TL whereas empty dots stand for a F4TCNQ 10 wt % doped TL.

The aim of this paper is to introduce easy-to-use guidelines for the optimization of the TLs in terms of thickness, mobility, and doping. In fact, one of the most common strategies to tackle the problem of the TL low mobilities is to use chemical doping. While it had been experimentally shown[13,16,19,28,32] that doping the TLs is an efficient way of improving the performance of PSCs, there are still questions that remain about the efficacy of this strategy. For instance, what is the best approach to improve the TL: increasing the TL mobility, reducing the thickness, or doping? Moreover, the general conditions to sufficiently dope a TL to achieve maximum photovoltaic performance depending on the layer thickness and mobility remain an important question today.

To this end, the roles of TL mobility, thickness, and doping have been examined through extensive drift-diffusion (DD) simulations that are based on a validated device model.[33] The simulation results are corroborated by transient extraction experiments which were conducted on two device structures consisting of the same highly efficient triple-cation perovskite layer but with different TL and device polarity ($n-i-p$ and $p-i-n$). Notably, the current–voltage characteristics of our $p-i-n$ devices could be well-reproduced with the numerical simulations. Both simulations and experiments show that doping clearly improves the efficiency of PSCs but also that increasing the mobility of the TL is a more efficient approach to maximize the collection efficiency with the additional benefit of avoiding a potential additional degradation pathway

due to the chemical dopant. Finally, we introduce a figure of merit solely based on the conductivity and thickness of the TLs so transport losses can be minimized.

The typical TLs used in PSCs such as 2,2',7,7'tetrakis[N,N-di(4-methoxyphenyl)amino]9,9'-spirobifluorene (spiro-OMe-TAD), poly(3hexylthiophene-2,5-diyl) (P3HT), poly[bis-(4phenyl)(2,4,6-trimethylphenyl)amine] (PTAA), and [6,6]-phenyl-C71-butyric acid methyl ester (PCBM), to name just a few, have mobilities which are generally more than 3 orders of magnitude lower than that of the perovskite and are usually 10 to over 150 nm thick.[15,34,35] The mobility and thickness of the TL strongly impact the charge transport/extraction in PSCs and end up drastically reducing the fill-factor (FF).[15,28]

In this study, two sets of devices were investigated both based on the same active layer made of a highly efficient triple-cation perovskite[26,29] in the $p-i-n$ or $n-i-p$ layout, as shown in Figure 1a,d. Both devices consist of a C_{60} layer as the electron transport layer (ETL). For the $p-i-n$ structure the hole transport layer (HTL) thickness, made of PTAA, was varied and/or also doped using a small molecule (2,3,5,6-tetrafluoro-2,5cyclohexadiene-1,4-diylidene)dimalononitrile (F4TCNQ). Similarly, the HTL thickness of the $n-i-p$ devices made of P3HT was also varied and doped using F4TCNQ. The 10 nm thick PTAA device demonstrated the highest performance reaching 20%. The current density versus voltage ($J-V$) curves (Figure 1b,e) show that the open-circuit voltage (V_{oc}) and the short-circuit current (J_{sc}) are not affected
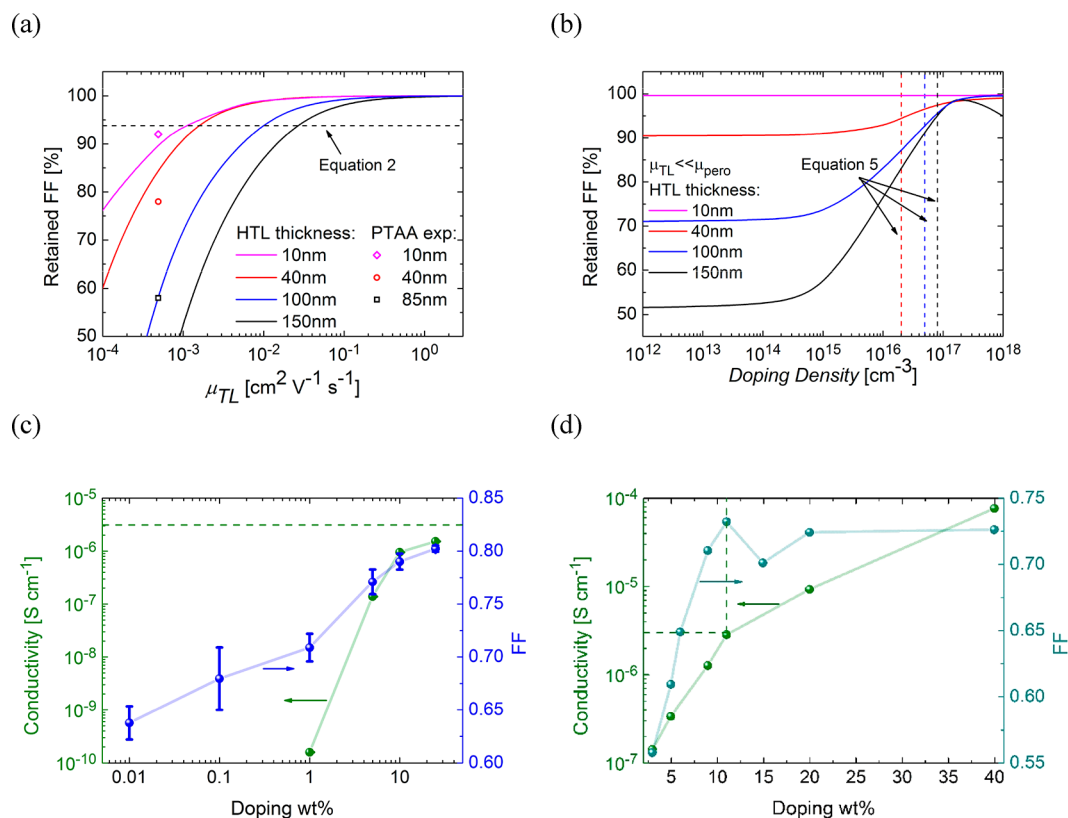
Figure 2. Simulations (a) show that reducing the mobility of the TLs drastically reduces the FF; however, simulations (b) and the experimental results on our PTAA devices (c) and devices from the literature (d, taken from ref 32) also show that this effect can be almost balanced by significant TL doping. The retained FF stands for the ratio between the considered FF over the FF when using a pristine high-mobility TL. The dashed line in part a is a guide to the eye to judge which points satisfy eq 2. The dashed lines in part b correspond to the values calculated with eq 5. The simulation parameters can be found in the simulation section in the SI.

by the change in thickness or by the doping of the TL, the small loss in J_{sc} is due to optical losses. However, the FF is strongly affected by both thickness and doping of the TL; the FF linearly decreases with the increase of the TL thickness and increases upon doping (see Figure 1).

To gain some insight in the effect of TL properties on the FF, a home-built device model based on 1-dimensional DD equations is used.[33,36] Employing steady-state DD simulations permits the calculation of current–voltage characteristics, by solving the Poisson and continuity equations (see the simulation section in the Supporting Information (SI) for more details). The simulations allow the disentangling of the influence of a single parameter from others, which is difficult to realize in the experiment, and give us a better understanding of the effect of a certain parameter on the solar cell performance. Our device model has already been validated[33,36] and accurately reproduces PSCs with a different composition and structure. The accuracy of the device model is demonstrated here once again as it perfectly reproduces the behavior of the PTAA devices as seen in Figure 1b. The DD fit also shows that trap-assisted recombination at the interface between the perovskite and the TLs is the dominant recombination loss (see Table S2). This is in agreement with previous reports on the losses in PSCs with various device architectures, processing methods, and perovskite compositions.[26,33,36,37] It thus appears that the dominance of interfacial recombination is a general rule in highly efficient PSCs stressing the importance of improved TLs.

The simulation results in Figure 2a are obtained by varying only the mobility and/or the thickness of a pristine (i.e., not doped) TL (see the simulation section in the SI for details). The linear dependence of the FF with the TL thickness is observed (see Figure S1a) which goes hand in hand with the experimental results. Figure 2a shows that, for mobilities on the order of 10^{-4} to 10^{-3} cm^2 V^{-1} s^{-1} and thicknesses of 10−150 nm, which are typical for most TLs and especially the organic ones, only ≈50−75% of the FF is retained, meaning that about 25−50% of the FF is lost just because of the poor transport in the TLs. Note that the retained FF in Figure 2 stands for the ratio between the actual FF and the maximum FF for the high-mobility TL. This effect, of course, becomes less critical when very thin TLs are used; however, experimentally the use of such a thin layer (<10−20 nm) is challenging and can result in less efficient or stable devices because of the formation of a pinhole or bad surface properties. To summarize, reducing the mobility and increasing the thickness of the TL are highly detrimental to the FF. Grill et al.[15] also showed that the transit time (t_{tr}) of the PSC is strongly affected by the t_{tr} of the TL whereas, ideally, the t_{tr} should only depend on the active material. As a first estimate, the charge transport quality of a pristine TL (i.e., not doped) can be defined as the ratio between the transit time in the TL over the perovskite. The transit time can be written as

$$t_{tr} = \frac{l}{\mu \times F} \tag{1}$$

with l the thickness, μ the mobility, and F the electrical field; the electrical field can also be approximated to V/l with V being the voltage drop. The simulation shows that the FF loss is acceptable when

$$\frac{t_{tr}^{TL}}{t_{tr}^{pero}} = \frac{l_{TL}^2 \times \mu_{pero}}{L_{pero}^2 \times \mu_{TL}} \lesssim 1 \tag{2}$$

as shown in Figure 2a. Indeed, when eq 2 is satisfied the transport losses due to the TL become negligible. A wide range of simulations with randomly picked parameters within a reasonable range describing the PSC behavior (see the SI) also show that when eq 2 holds the FF is not affected by the TL. However, when eq 2 is not satisfied the FF is reduced.

If we consider a TL of 40 nm and a 300 nm perovskite layer with a mobility of 1 cm^2 V^{-1} s^{-1}, which is typical for PSCs, the required TL mobility to avoid FF losses is 0.01 cm^2 V^{-1} s^{-1}, which is the same number as that found by Tessler and Vaynzof in ref 38.

Consequently, the use of high mobility and/or very thin TLs seems to be required to guarantee high efficiency. Equation 2 also gives us a good criterion to optimize the TL thickness and gives a threshold to judge whether doping the TL is required.

As mentioned above, one other way to tackle the issue of the TL low mobility is to use doped TLs which help to maintain a high performance. In fact, chemical doping of organic TLs[16,32,39] and atomic doping of oxides[19,40] have proven to be a successful strategy to counterbalance the poor transport properties of many TLs. While knowing that doping is, in general, a good strategy to improve the efficiency, the question of how much the TL needs to be doped to reach the best performance still remains. One of the main resulting effects of doping the TL is to increase its conductivity. Note that increasing the mobility as discussed previously also increases the conductivity. Ohm's law can be rewritten in terms of conductivity such that the voltage drop within the TL can be quantified as

$$V = R \times I = \frac{l \times J}{\sigma} \tag{3}$$

with V the voltage drop, R the resistance, I (J) the current (density), l the thickness, and σ the conductivity. We assume that the TLs will have a negligible influence if the voltage drop across a TL is equal or less than the thermal voltage V_T, which is a reasonable assumption as carriers ought to be able to overcome a potential drop equivalent to kT in energy. Below, this assumption is confirmed by both simulations and experiments. The largest current that a solar cell supplies is equal to the short-circuit current density J_{sc}, so we require that

$$\sigma = q\mu_{TL}N_D \geq \frac{l_{TL} \times J_{sc}}{V_T} \tag{4}$$

Equation 4 gives us a new and easily accessible criterion on the required conductivity for an efficient TL; it also makes it easier to select and optimize a TL even before making the PSC full stack. For example, if we consider a 40 nm thick TL and a J_{sc} of 20 mA cm^{-2}, which are typical for perovskite solar cells, then we need a TL conductivity of at least 3×10^{-6} S cm^{-1}. Equation 4 can also be rewritten in terms of doping density such as

$$N_D = \frac{l_{TL} \times J_{sc}}{qV_T\mu_{TL}} \tag{5}$$

Following this idea, the simulations were performed again including some doping of the TL to determine if the efficiency can be fully recovered and how much the TL needs to be doped. Two cases were studied with one thin (40 nm) and one thick (150 nm) HTL—similar results would be obtained if the ETL was studied—and the doping density within the TL was increased until the best performance is reached. In both cases, more than 95% of the FF is retained when using eq 5 and is very close to the maximum FF that can be reached by doping (see Figure 2). In addition, in a large-scale simulation of perovskite solar cells (see Figure S1c), more than 10 000 different solar cells were simulated to evaluate the accuracy of eqs 4 and 5. In this simulation, the different relevant parameters of a PSC were varied such as device thickness, mobilities, and trapping densities (see Table S2). Note that, to disentangle the effect of doping one TL, only one of the two TLs was set as "defective" in the simulations (i.e., with a low mobility) whereas the other one was considered as "perfect" (i.e., with high mobility), and only the defective TL was then doped. In this simulation both the hole and electron TLs were alternatively considered as the defective one showing that this approach is relevant for both electron and hole TLs. In more than 90% of cases doping the TL helps to recover the FF loss due to the low TL mobility; therefore, eqs 4 and 5 indeed give an accurate description of the optimal doping.

The effect of doping the TL was studied in the case of the PTAA devices, where the concentration of the F4TCNQ dopant in a 40 nm thick PTAA layer was varied between 0.01 and 25 wt % (see Figure 2c). The conductivity of the doped PTAA was also measured for the different doping concentration; however, it is important to note that the conductivity of the TL within the solar cell stack matters in eq 4, and therefore, one has to be careful on how to measure this experimentally. In fact, as the perovskite layer is spin-cast on top of the PTAA layer the solvent (DMF:DMSO) might wash some of the F4TCNQ anions or PTAA away hence reducing the conductivity or thickness. To mimic this "washing effect" the conductivities were measured as-cast and after spin coating a solution of DMF:DMSO following the same procedure as if it was the perovskite solution. On one hand, the layer thickness was measured for both as-cast and washed films to see if there was PTAA washing as well, but the effect was negligible indicating that the PTAA is not washed away. On the other hand, a drop in conductivity by more than 2 orders of magnitude for washed films is measured (see Figure S2), which makes it evident that F4TCNQ anions are not present in the films at the initial desired concentration, lowering the doping efficiency and inevitably the free charge carrier density.

The measured conductivity after washing is reported in Figure 2c. The increase of the conductivity correlates very well with the increase in FF in a similar fashion to what is seen in the simulation. Unfortunately, the conductivity does not reach the required value from eq 4 of 3×10^{-6} S cm^{-1} (green dotted line in Figure 2c) which is coherent with the fact that the maximum FF does not seem to be achieved yet in this device. Above 10 wt % further increasing the dopant concentration only slightly increases the conductivity, and therefore, only a modest increase in the FF is observed; this is due to a bad mixing of the dopant with the PTAA which degrades the morphology. In the future, replacing F4TCNQ with another
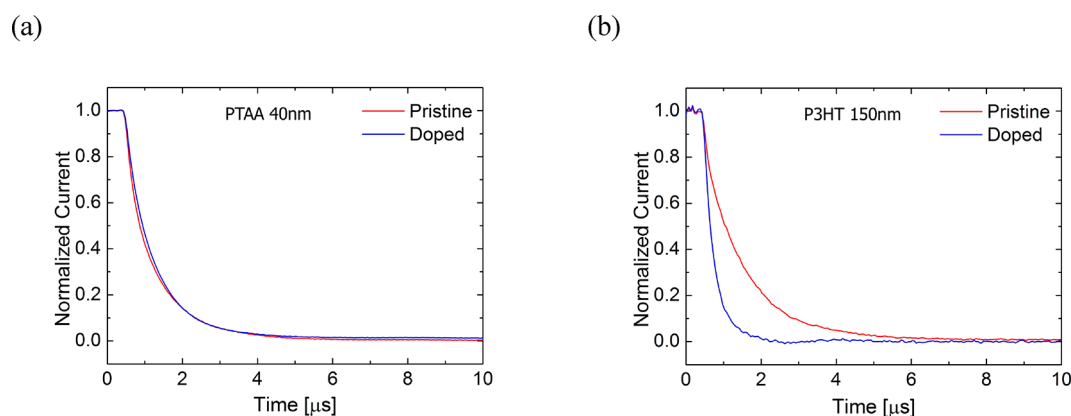
(a)   (b)

Figure 3. (a) In the photocurrent decay experiment, the extraction is not really affected by the doping for a thin 40 nm PTAA HTL. (b) However, for a thicker TL—here 150 nm thick P3HT HTL—the extraction is enhanced upon TL doping leading to a faster decay of the current density. The experiment is shown at short-circuit conditions.
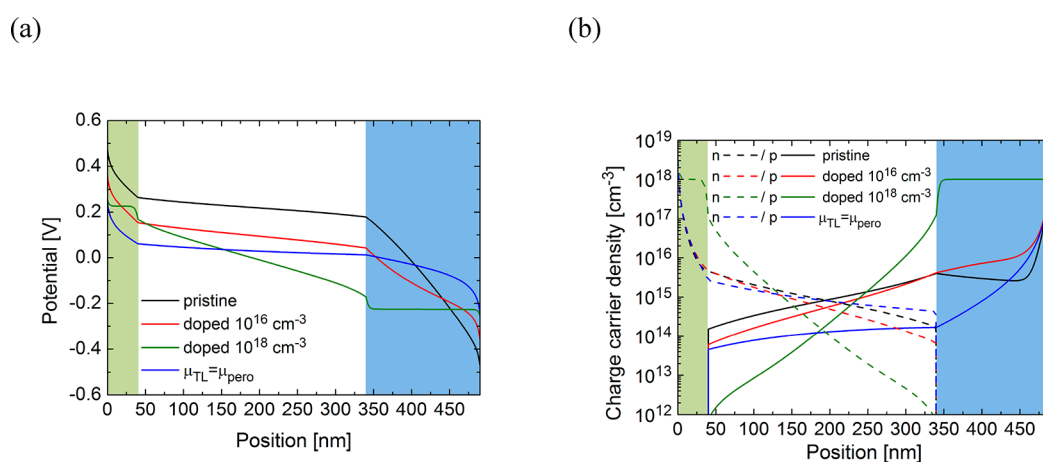
(a)   (b)

Figure 4. (a) Beneficial influence of TL doping that reduces the potential drop within the TL. (b) Upon doping there is less accumulation of charge carriers in the perovskite and more in the TL. Therefore, the extraction is enhanced when doping a low-mobility TL because there are more charge carriers that can be extracted next to the electrode which counterbalances the fact that they are slower. This explains why upon sufficient doping the extraction becomes almost as good as when using a high-mobility TL. The potential and charge carrier density profiles are here shown at the MPP. The simulation parameters can be found in the simulation section in the SI.

dopant or changing the solvent would be a good strategy to reach higher doping efficiencies and FFs.

The P3HT cells were also doped with F4TCNQ 10 wt % and show a significant improvement of the FF upon doping, especially the 150 nm thick devices that show an improvement of 175% and help to reach an FF similar to those of much thinner P3HT thickness devices (see Figure 1e−f). However, for those devices, the limitation in V_{oc} probably due to strong interfacial recombination seems to be limiting the performance more than the transport losses within the TL.[37]

A similar analysis was applied to fully vacuum-deposited devices based on methylammonium lead iodide (MAPbI$_3$) stacked between a N1,N4-bis(tri-p-tolylphosphoranylidene)-benzene-1,4-diamine (PhIm)-doped fullerene C$_{60}$ ETL and a 2,2′-(perfluoronaphthalene2,6-diylidene) dimalononitrile (F6-TCNNQ)-doped N4,N4,N4″,N4″-tetra([1,1′-biphenyl]4-yl)-[1,1′:4′,1″-terphenyl]-4,4″-diamine (TaTm) HTL (see ref 32 for full device structures). Reference 32 concluded that the ETL was not limiting the FF which is coherent with eq 4 giving 3×10^{-6} S cm^{-1} (for a 40 nm TL) which is lower than the measured conductivity of the ETL above 2×10^{-4} S cm^{-1}, showing again that eq 4 can also be applied for the ETL. The HTL, however, has a rather low conductivity $\approx 1 \times 10^{-7}$ S

cm^{-1} and needs to be significantly doped to recover a high performance. The maximum efficiency (see Figure 2d) is reached for an 11 wt % F6-TCNNQ doping and a conductivity of 3×10^{-6} S cm^{-1} which coincides perfectly with the value expected from eq 4. As the layers were all vacuum-processed, there is no need to consider any washing effect. At a higher doping concentration, even though the conductivity still significantly increases, the FF is not so much affected just as shown by the simulation meaning that the TL is now fully optimized in terms of transport and that the conductivity criterion presented here is accurate. However, the FF is still not ideal, but this can probably be explained by the significant amount of recombination which tends to limit the FF in this system as shown in ref 36.

An increase in FF can be related to two processes: a more efficient extraction or a reduced number of recombination pathways.[41] To further understand the effect of TL thickness and doping on the extraction dynamics of PSCs, a photo-current decay experiment, similar to the one described in ref 42, was set up. The device is kept under 1 sun illumination, using white light, to establish steady state operating conditions. At time zero the light intensity is slightly reduced, and the current decay is monitored over time giving the extraction rate

by fitting a monoexponential decay.[42] When the decay rate k is higher, i.e. shorter lifetime, the extraction is better.

This experiment can be done at a different applied voltage that is kept constant during the light reduction. The behavior of two devices was studied, one PTAA cell with a thin HTL of 40 nm and one P3HT cell with a thick HTL of 150 nm. The HTLs of the two devices were then doped with 10 wt % F4TCNQ. In the case of a thin 40 nm PTAA TL (see Figure 3a), the experiment shows that the extraction is not significantly affected by the doping of the TL. However, the experiment on a thick 150 nm P3HT device (b) shows that doping plays a major role in the extraction. The decay of the current is much faster for a doped TL than for its pristine counterpart (see Figure 3b).

Transient simulations were also performed (see Figure S4) for both a thin and thick TL, with a TL mobility of 10^{-3} cm^2 V^{-1} s^{-1}; they also show that doping has little effect on the extraction time for the thin TL but leads to a significant improvement of the extraction of thick TLs. In addition, the simulations using the high-mobility TL show that it always leads to the fastest extraction which is coherent with the higher FF reported in Figure 2 when using the higher-mobility TL.

While it is straightforward that the extraction becomes more efficient when the TL mobility is increased, charge carriers just move faster; it is not so clear how doping helps in the case of low mobility. The simulations in Figure 4a,b highlight the two concomitant benefits of doping a low-mobility TL: on one hand it decreases the potential drop in the TL—as referred to in the derivation of eqs 4 and 5—which results in a bigger potential drop within the perovskite layer and so to a higher electrical field (corresponding energy diagrams are available in the SI). Note that the data in Figure 4 correspond to the maximum power point (MPP) values as this is the meaningful operating point for solar cells; this explains the fact that the overall potential drop varies from one simulation to the next as V_{MPP} is different. On the other hand, the charge carrier density within the perovskite is greatly reduced while the concentration in the TL increases tremendously. These two synergic effects explain why the current decays faster in the transient photocurrent experiment when a low-mobility TL is doped. Under steady-state illumination, most charge carriers are close to their extracting electrode (see Figure 4b), so when the light is slightly reduced the carriers that were already there do not have to travel far to be extracted.

Another side effect of doping is that the lower carrier concentration within the perovskite also reduces the total amount of recombination (see Figure S5), for both the thin and thick TL. It could explain why for a thin TL even though the extraction is not so much affected the FF still increases by 10% for the 40 nm PTAA device (see Figure 1c). For the 150 nm P3HT device the FF shows a huge increase of 175% because it benefits from the two effects, enhanced extraction and lower recombination. It is worth noting that the thick pristine P3HT TL devices (see Figure S3) show a very strong voltage dependence of the extraction rate and also of the ratio of initial and final currents (see Figure S3d), which is a sign of a substantial effect of recombination. The decay rate of the doped system tends to be way less affected by the applied voltage and , hence, is less dominated by recombination which goes hand in hand with the previous conclusion.

Finally, all the above-mentioned points demonstrate that the approach presented earlier of reducing the voltage drop within

the TL is indeed crucial and that the criterion presented here is a key parameter to achieve high efficiency.

So far we have only talked about organic TLs; however, all the reasoning described above is applicable for inorganic TLs, but in most cases, the inorganic TLs such as TiO$_2$[40,43−45] or SnO$_2$[23,46] have conductivities close[40,46] to our criterion or above hence leading to only modest improvement of the FF. The main reason for the performance improvement in those cases is likely due to either trap-passivation or better energy level alignment showing up in an improved open-circuit voltage.

To summarize, the experiments and simulations consistently show that the extraction and consequently the FF are limited by the TL in common PSCs using a low-mobility TL that are not appropriately doped. Thus, if low-mobility TLs have to be used because of a lack of good alternatives, then they need to be doped following the conductivity criterion described by eq 4. Doping the TL remains a very efficient approach of reaching high efficiencies when using low mobility, but the best case scenario is always the case of the thin TL with high mobility.

In conclusion, simulation and experimental results were combined to show that transport layers are a limiting factor in the efficiency of perovskite solar cells. The low mobility of commonly used transport layers not only limits the extraction but also increases recombination. To counterbalance this effect two strategies can be used: doping the transport layer or using different materials with higher mobility. These two options are both viable and lead to high efficiency, but using doping might lead to other issues such as parasitic absorption from the dopant, dopant diffusion, and additional degradation pathways. Hence, finding new materials with high mobility appears to be the best strategy.

Two new and simple criteria are introduced to help tune the transport layer thickness and/or conductivity to reach a high efficiency. The first criterion helps to optimize the thickness of the transport layer and judge whether doping is required. The second criterion ensures that the TL conductivity is sufficient to ensure good transport. These criteria can be used prior to the fabrication of the full solar cells and will help to save time, materials, and money in future optimization work.

■ ASSOCIATED CONTENT

ⓢ Supporting Information

The Supporting Information is available free of charge on the ACS Publications website at DOI: 10.1021/acsaem.9b00856.

> Further details and results on the simulation and experiments (PDF)

■ AUTHOR INFORMATION

Corresponding Authors
*E-mail: v.m.lecorre@rug.nl.
*E-mail: l.j.a.koster@rug.nl.
ORCID ⓘ
Vincent M. Le Corre: 0000-0001-6365-179X
Martin Stolterfoht: 0000-0002-4023-2178
Christian Wolff: 0000-0002-7210-1869
Henk J. Bolink: 0000-0001-9784-6253
Dieter Neher: 0000-0001-6618-8403
L. Jan Anton Koster: 0000-0002-6558-5295

■ REFERENCES

(1) Kojima, A.; Teshima, K.; Shirai, Y.; Miyasaka, T. Organometal Halide Perovskites as Visible-Light Sensitizers for Photovoltaic Cells. *J. Am. Chem. Soc.* **2009**, *131* (17), 6050−6051.

(2) NREL. Best Research-Cell Efficiencies. https://www.nrel.gov/pv/assets/images/efficiency-chart.png (accessed July 2019).

(3) Kim, H.-S.; Lee, C.-R.; Im, J.-H.; Lee, K.-B.; Moehl, T.; Marchioro, A.; Moon, S.-J.; Humphry-Baker, R.; Yum, J.-H.; Moser, J. E.; Grätzel, M.; Park, N.-G. Lead Iodide Perovskite Sensitized All-Solid-State Submicron Thin Film Mesoscopic Solar Cell with Efficiency Exceeding 9%. *Sci. Rep.* **2012**, *2* (1), 591.

(4) Lee, M. M.; Teuscher, J.; Miyasaka, T.; Murakami, T. N.; Snaith, H. J. Efficient Hybrid Solar Cells Based on Meso-Superstructured Organometal Halide Perovskites. *Science (Washington, DC, U. S.)* **2012**, *338* (6107), 643−647.

(5) Bi, D.; Moon, S.-J.; Häggman, L.; Boschloo, G.; Yang, L.; Johansson, E. M. J.; Nazeeruddin, M. K.; Grätzel, M.; Hagfeldt, A. Using a Two-Step Deposition Technique to Prepare Perovskite ($CH_3NH_3PbI_3$) for Thin Film Solar Cells Based on ZrO_2 and TiO_2 Mesostructures. *RSC Adv.* **2013**, *3* (41), 18762.

(6) Nie, W.; Tsai, H.; Asadpour, R.; Blancon, J.-C.; Neukirch, A. J.; Gupta, G.; Crochet, J. J.; Chhowalla, M.; Tretiak, S.; Alam, M. A.; Wang, H.-L.; Mohite, A. D. High-Efficiency Solution-Processed Perovskite Solar Cells with Millimeter-Scale Grains. *Science (Washington, DC, U. S.)* **2015**, *347* (6221), 522−525.

(7) Pérez-del-Rey, D.; Boix, P. P.; Sessolo, M.; Hadipour, A.; Bolink, H. J. Interfacial Modification for High-Efficiency Vapor-Phase-Deposited Perovskite Solar Cells Based on a Metal Oxide Buffer Layer. *J. Phys. Chem. Lett.* **2018**, *9* (5), 1041−1046.

(8) Jeon, N. J.; Noh, J. H.; Yang, W. S.; Kim, Y. C.; Ryu, S.; Seo, J.; Seok, S. Il Compositional Engineering of Perovskite Materials for High-Performance Solar Cells. *Nature* **2015**, *517* (7535), 476−480.

(9) Saliba, M.; Matsui, T.; Seo, J.-Y.; Domanski, K.; Correa-Baena, J.-P.; Nazeeruddin, M. K.; Zakeeruddin, S. M.; Tress, W.; Abate, A.; Hagfeldt, A.; Grätzel, M. Cesium-Containing Triple Cation Perovskite Solar Cells: Improved Stability, Reproducibility and High Efficiency. *Energy Environ. Sci.* **2016**, *9* (6), 1989−1997.

(10) Deng, Y.; Dong, Q.; Bi, C.; Yuan, Y.; Huang, J. Air-Stable, Efficient Mixed-Cation Perovskite Solar Cells with Cu Electrode by Scalable Fabrication of Active Layer. *Adv. Energy Mater.* **2016**, *6* (11), 1600372.

(11) Prasanna, R.; Gold-Parker, A.; Leijtens, T.; Conings, B.; Babayigit, A.; Boyen, H.-G.; Toney, M. F.; McGehee, M. D. Band Gap Tuning via Lattice Contraction and Octahedral Tilting in Perovskite Materials for Photovoltaics. *J. Am. Chem. Soc.* **2017**, *139* (32), 11117−11124.

(12) Momblona, C.; Gil-Escrig, L.; Bandiello, E.; Hutter, E. M.; Sessolo, M.; Lederer, K.; Blochwitz-Nimoth, J.; Bolink, H. J. Efficient Vacuum Deposited P−i−n and n−i−p Perovskite Solar Cells Employing Doped Charge Transport Layers †. *Energy Environ. Sci.* **2016**, *9*, 3456−3463.

(13) Chen, W.; Liu, F.-Z.; Feng, X.-Y.; Djurišić, A. B.; Chan, W. K.; He, Z.-B. Cesium Doped NiO_x as an Efficient Hole Extraction Layer for Inverted Planar Perovskite Solar Cells. *Adv. Energy Mater.* **2017**, *7* (19), 1700722.

(14) Chen, H.; Fu, W.; Huang, C.; Zhang, Z.; Li, S.; Ding, F.; Shi, M.; Li, C.-Z.; Jen, A. K.-Y.; Chen, H. Molecular Engineered Hole-Extraction Materials to Enable Dopant-Free, Efficient p−i−n Perovskite Solar Cells. *Adv. Energy Mater.* **2017**, *7* (18), 1700012.

(15) Grill, I.; Aygüler, M. F.; Bein, T.; Docampo, P.; Hartmann, N. F.; Handloser, M.; Hartschuh, A. Charge Transport Limitations in Perovskite Solar Cells: The Effect of Charge Extraction Layers. *ACS Appl. Mater. Interfaces* **2017**, *9* (43), 37655−37661.

(16) Wang, Z.; McMeekin, D. P.; Sakai, N.; van Reenen, S.; Wojciechowski, K.; Patel, J. B.; Johnston, M. B.; Snaith, H. J. Efficient and Air-Stable Mixed-Cation Lead Mixed-Halide Perovskite Solar Cells with n-Doped Organic Electron Extraction Layers. *Adv. Mater.* **2017**, *29* (5), 1604186.

(17) Wu, W.-Q.; Chen, D.; Caruso, R. A.; Cheng, Y.-B. Recent Progress in Hybrid Perovskite Solar Cells Based on N-Type Materials. *J. Mater. Chem. A* **2017**, *5* (21), 10092−10109.

(18) Fang, R.; Wu, S.; Chen, W.; Liu, Z.; Zhang, S.; Chen, R.; Yue, Y.; Deng, L.; Cheng, Y.-B.; Han, L.; Chen, W. [6,6]-Phenyl-C_{61}-Butyric Acid Methyl Ester/Cerium Oxide Bilayer Structure as Efficient and Stable Electron Transport Layer for Inverted Perovskite Solar Cells. *ACS Nano* **2018**, *12* (3), 2403−2414.

(19) Sidhik, S.; Cerdan Pasarán, A.; Esparza, D.; López Luke, T.; Carriles, R.; De la Rosa, E. Improving the Optoelectronic Properties of Mesoporous TiO_2 by Cobalt Doping for High-Performance Hysteresis-Free Perovskite Solar Cells. *ACS Appl. Mater. Interfaces* **2018**, *10* (4), 3571−3580.

(20) Zhao, X.; Tao, L.; Li, H.; Huang, W.; Sun, P.; Liu, J.; Liu, S.; Sun, Q.; Cui, Z.; Sun, L.; Shen, Y.; Yang, Y.; Wang, M. Efficient Planar Perovskite Solar Cells with Improved Fill Factor via Interface Engineering with Graphene. *Nano Lett.* **2018**, *18* (4), 2442−2449.

(21) Ouyang, D.; Xiao, J.; Ye, F.; Huang, Z.; Zhang, H.; Zhu, L.; Cheng, J.; Choy, W. C. H. Strategic Synthesis of Ultrasmall $NiCo_2O_4$ NPs as Hole Transport Layer for Highly Efficient Perovskite Solar Cells. *Adv. Energy Mater.* **2018**, *8* (16), 1702722.

(22) Pham, H. D.; Do, T. T.; Kim, J.; Charbonneau, C.; Manzhos, S.; Feron, K.; Tsoi, W. C.; Durrant, J. R.; Jain, S. M.; Sonar, P. Molecular Engineering Using an Anthanthrone Dye for Low-Cost Hole Transport Materials: A Strategy for Dopant-Free, High-Efficiency, and Stable Perovskite Solar Cells. *Adv. Energy Mater.* **2018**, *8* (16), 1703007.

(23) Yang, G.; Chen, C.; Yao, F.; Chen, Z.; Zhang, Q.; Zheng, X.; Ma, J.; Lei, H.; Qin, P.; Xiong, L.; Ke, W.; Li, G.; Yan, Y.; Fang, G. Effective Carrier-Concentration Tuning of SnO_2 Quantum Dot Electron-Selective Layers for High-Performance Planar Perovskite Solar Cells. *Adv. Mater.* **2018**, *30* (14), 1706023.

(24) Schulz, P.; Edri, E.; Kirmayer, S.; Hodes, G.; Cahen, D.; Kahn, A. Interface Energetics in Organo-Metal Halide Perovskite-Based Photovoltaic Cells. *Energy Environ. Sci.* **2014**, *7* (4), 1377.

(25) Polander, L. E.; Pahner, P.; Schwarze, M.; Saalfrank, M.; Koerner, C.; Leo, K. Hole-Transport Material Variation in Fully Vacuum Deposited Perovskite Solar Cells. *APL Mater.* **2014**, *2* (8), No. 081503.

(26) Stolterfoht, M.; Wolff, C. M.; Márquez, J. A.; Zhang, S.; Hages, C. J.; Rothhardt, D.; Albrecht, S.; Burn, P. L.; Meredith, P.; Unold, T.; Neher, D. Visualization and Suppression of Interfacial Recombination for High-Efficiency Large-Area Pin Perovskite Solar Cells. *Nat. Energy* **2018**, *3* (10), 847−854.

(27) Zhang, S.; Stolterfoht, M.; Armin, A.; Lin, Q.; Zu, F.; Sobus, J.; Jin, H.; Koch, N.; Meredith, P.; Burn, P. L.; Neher, D. Interface Engineering of Solution-Processed Hybrid Organohalide Perovskite Solar Cells. *ACS Appl. Mater. Interfaces* **2018**, *10* (25), 21681−21687.

(28) Marinova, N.; Tress, W.; Humphry-Baker, R.; Dar, M. I.; Bojinov, V.; Zakeeruddin, S. M.; Nazeeruddin, M. K.; Grätzel, M. Light Harvesting and Charge Recombination in $CH_3NH_3PbI_3$ Perovskite Solar Cells Studied by Hole Transport Layer Thickness Variation. *ACS Nano* **2015**, *9* (4), 4200−4209.

(29) Stolterfoht, M.; Wolff, C. M.; Amir, Y.; Paulke, A.; Perdigón-Toro, L.; Caprioglio, P.; Neher, D. Approaching the Fill Factor Shockley−Queisser Limit in Stable, Dopant-Free Triple Cation Perovskite Solar Cells. *Energy Environ. Sci.* **2017**, *10* (6), 1530−1539.

(30) Maddalena, F.; Boix, P. P.; Xin Yu, C.; Mathews, N.; Soci, C.; Mhaisalkar, S. Charge Transport in Organometal Halide Perovskites. In *Organic-Inorganic Halide Perovskite Photovoltaics*; Springer International Publishing: Cham, 2016; pp 201−222.

(31) Herz, L. M. Charge-Carrier Mobilities in Metal Halide Perovskites: Fundamental Mechanisms and Limits. *ACS Energy Lett.* **2017**, *2* (7), 1539−1548.

(32) Momblona, C.; Gil-Escrig, L.; Bandiello, E.; Hutter, E. M.; Sessolo, M.; Lederer, K.; Blochwitz-Nimoth, J.; Bolink, H. J. Efficient Vacuum Deposited P−i−n and n−i−p Perovskite Solar Cells Employing Doped Charge Transport Layers. *Energy Environ. Sci.* **2016**, *9* (11), 3456−3463.

(33) Sherkar, T. S.; Momblona, C.; Gil-Escrig, L.; Bolink, H. J.; Koster, L. J. A. Improving Perovskite Solar Cells: Insights From a Validated Device Model. *Adv. Energy Mater.* **2017**, *7* (13), 1602432.

(34) Vivo, P.; Salunke, J.; Priimagi, A.; Vivo, P.; Salunke, J. K.; Priimagi, A. Hole-Transporting Materials for Printable Perovskite Solar Cells. *Materials* **2017**, *10* (9), 1087.

(35) Jiménez-López, J.; Cambarau, W.; Cabau, L.; Palomares, E. Charge Injection, Carriers Recombination and HOMO Energy Level Relationship in Perovskite Solar Cells. *Sci. Rep.* **2017**, *7* (1), 6101.

(36) Sherkar, T. S.; Momblona, C.; Gil-Escrig, L.; Ávila, J.; Sessolo, M.; Bolink, H. J.; Koster, L. J. A. Recombination in Perovskite Solar Cells: Significance of Grain Boundaries, Interface Traps, and Defect Ions. *ACS Energy Lett.* **2017**, *2* (5), 1214−1222.

(37) Stolterfoht, M.; Caprioglio, P.; Wolff, C. M.; Márquez, J. A.; Nordmann, J.; Zhang, S.; Rothhart, D.; Hörmann, U.; Redinger, A.; Kegelmann, L.; Albrecht, S.; Kirchartz, T.; Saliba, M.; Unold, T.; Neher, D. The perovskite/transport layer interfaces dominate non-radiative recombination in efficient perovskite solar cells. 2018, arXiv:1810.01333. arXiv.org e-Print archive. http://arxiv.org/abs/1810.01333 (accessed Oct 16, 2018).

(38) Tessler, N.; Vaynzof, Y. Preventing Hysteresis in Perovskite Solar Cells by Undoped Charge Blocking Layers. *ACS Appl. Energy Mater.* **2018**, *1* (2), 676−683.

(39) Liu, D.; Li, Y.; Yuan, J.; Hong, Q.; Shi, G.; Yuan, D.; Wei, J.; Huang, C.; Tang, J.; Fung, M.-K. Improved Performance of Inverted Planar Perovskite Solar Cells with F4-TCNQ Doped PEDOT:PSS Hole Transport Layers. *J. Mater. Chem. A* **2017**, *5* (12), 5701−5708.

(40) Yin, G.; Ma, J.; Jiang, H.; Li, J.; Yang, D.; Gao, F.; Zeng, J.; Liu, Z.; Liu, S. F. Enhancing Efficiency and Stability of Perovskite Solar Cells through Nb-Doping of TiO_2 at Low Temperature. *ACS Appl. Mater. Interfaces* **2017**, *9* (12), 10752−10758.

(41) Bartesaghi, D.; Perez, I. d. C.; Kniepert, J.; Roland, S.; Turbiez, M.; Neher, D.; Koster, L. J. A. Competition between Recombination and Extraction of Free Charges Determines the Fill Factor of Organic Solar Cells. *Nat. Commun.* **2015**, *6*, 7083.

(42) Le Corre, V. M.; Chatri, A. R.; Doumon, N. Y.; Koster, L. J. A. Charge Carrier Extraction in Organic Solar Cells Governed by Steady-State Mobilities. *Adv. Energy Mater.* **2017**, *7* (22), 1701138.

(43) Peng, J.; Duong, T.; Zhou, X.; Shen, H.; Wu, Y.; Mulmudi, H. K.; Wan, Y.; Zhong, D.; Li, J.; Tsuzuki, T.; Weber, K. J.; Catchpole, K. R.; White, T. P. Efficient Indium-Doped TiO_x Electron Transport Layers for High-Performance Perovskite Solar Cells and Perovskite-Silicon Tandems. *Adv. Energy Mater.* **2017**, *7* (4), 1601768.

(44) Wang, S.; Liu, B.; Zhu, Y.; Ma, Z.; Liu, B.; Miao, X.; Ma, R.; Wang, C. Enhanced Performance of TiO_2-Based Perovskite Solar Cells with Ru-Doped TiO_2 Electron Transport Layer. *Sol. Energy* **2018**, *169*, 335−342.

(45) Gu, X.; Wang, Y.; Zhang, T.; Liu, D.; Zhang, R.; Zhang, P.; Wu, J.; Chen, Z. D.; Li, S. Enhanced Electronic Transport in Fe^{3+}-Doped TiO_2 for High Efficiency Perovskite Solar Cells. *J. Mater. Chem. C* **2017**, *5* (41), 10754−10760.

(46) Zhou, N.; Cheng, Q.; Li, L.; Zhou, H. Doping Effects in SnO_2 Transport Material for High Performance Planar Perovskite Solar Cells. *J. Phys. D: Appl. Phys.* **2018**, *51* (39), 394001.